Defective Follicular Exclusion of Apoptotic Antigens Due to Marginal Zone Macrophage Defects in Autoimmune BXD2 Mice

Hao Li[*,†], **Qi Wu**[*], **Jun Li**[*], **PingAr Yang**[*], **Zilu Zhu**[‡], **Bao Luo**[*], **Hui-Chen Hsu**[*], and **John D Mountz**[*,†,§]

[*]Division of Clinical Immunology and Rheumatology, Department of Medicine, University of Alabama at Birmingham, Birmingham, AL

[†]Department of Microbiology, University of Alabama at Birmingham, Birmingham, AL

[‡]Division of Hematology & Oncology, Department of Medicine, University of Alabama at Birmingham, Birmingham, AL

[§]Birmingham VA Medical Center, Birmingham, AL, 35294

Abstract

Marginal zone macrophages (MZMs) act as a barrier to entry of circulating apoptotic debris into the follicles of secondary lymphoid organs. In autoimmune BXD2 mice, there is a progressive reduction in the function and numbers of MZMs. Absence of MZMs results in retention of apoptotic cell debris within the MZ and increased loading of apoptotic cell antigens on MZ B cells and MZ-precursor (MZ-P) B cells. The MZ-P B cells are capable of translocating the apoptotic cell antigens to the follicular zone and stimulating T cells. Both MZMs and MZ-P B cells from BXD2 mice express low levels of tolerogenic signals and high levels of inflammatory signals. Thus, the present study suggests a multifaceted mechanism in which MZMs maintain tolerance to apoptotic autoantigens and suppress their translocation to follicles. Lack of clearance of apoptotic debris by MZMs drives follicular Ag–transportation by MZ-P B cells to stimulate an autoimmune response.

Introduction

Apoptotic cells contain "blebs" which are highly enriched with autoantigens including nucleosomal DNA and small nuclear riboproteins (1, 2). Normally, the corpses of the apoptotic cells are removed locally by tissue macrophages (3). Apoptotic cells and debris that escape this clearance mechanism are prevented from entering the follicles of secondary lymphoid organs by the marginal zone (MZ). There is considerable evidence that loss of integrity of the MZ barrier that results in the lack of clearance of apoptotic cell autoantigens can contribute to development of autoimmune disease (4–8). The marginal zone macrophages (MZMs), which express the scavenger receptor SR-A and MARCO to sense and remove waste materials (8, 9), are a critical component of this barrier. In mice, autoimmune responses can be induced or promoted by either targeted deletion of SH2 domain-containing inositol 5′-phosphatase 1 (SHIP-1) in myeloid cells (9), which results in dislocations of MZMs, or treatment with an appropriate dose of clodronate liposome (CL), which results in loss of MZMs (5, 6).

Address correspondence and reprint requests to: Hui-Chen Hsu, PhD, and John D. Mountz, MD, 1825 University Blvd, Birmingham, AL 35294; Phone: 205-934-8909, Fax: 205-996-6788, rheu078@uab.edu; jdmountz@uab.edu.

BXD2 mice develop a lupus-like autoimmune disease (10). The generation of the high-affinity pathogenic autoantibodies is associated with the development of large spontaneous germinal centers (GCs) in the spleen (11–13). However, the mechanisms that permit the initial exposure of the B cells to the autoantigens have not yet been elucidated. The production of autoantibodies in BXD2 mice with specificity for Ags derived from a wide range of cellular compartments, including filament proteins, chromatin and ribonuclear components (14), is consistent with the concept that autoantigens can be derived by proteolytic cleavage during the process of apoptosis (1). The present results confirm that defective clearance of apoptotic debris by MZMs and the associated transport of apoptotic cell Ags by B cells can provoke a T-cell response in BXD2 mice.

Materials and Methods

Mice

Wild type C57BL/6 (B6), C57BL/6-Tg(TcraTcrb)425Cbn/J (OT-II TCR Tg), B6-$Rag2^{-/-}$, C57BL/6-Tg(CAG-OVA)916Jen/J transgenic mice expressing the membrane bound chicken ovalbumin on all cell surface (mOVA Tg) and BXD2 recombinant inbred mice were obtained from The Jackson Laboratory (Bar Harbor, ME); B6-$Rag2^{-/-}$ or B6-OT-II TCR Tg mice were backcrossed with BXD2 mice for > 10 generations to generate BXD2 OT-II TCR Tg or BXD2-$Rag2^{-/-}$ mice, which were further intercrossed to generate BXD2 OT-II TCR Tg $Rag2^{-/-}$ mice.

Apoptotic cells

For *in vivo* administration of apoptotic cells, mice were injected i.v. with 2×10^7 apoptotic thymocytes. For depletion of MZM, mice were treated i.v. with 150 μg of CL (Encapsula NanoSciences, Nashville, TN) 4 h before apoptotic cells transfer as described (5). Control mice were treated with PBS liposomes. The dose for selective delivery to MZMs was optimized by using Fluoroliposome (Encapsula NanoSciences).

CD4 T-cell stimulation

Splenic CD4 cells from BXD2 OT-II TCR Tg $Rag2^{-/-}$ mice were labeled with CFSE (5 μM) and transferred i.v. into recipient mice (2×10^6 per mouse). Recipient mice were administered apoptotic thymocytes prepared from mOVA Tg mice 12 h later and sacrificed after another 72 h.

In some experiments, red pulp macrophages (RPMs) (F4/80$^+$CD11b^{lo}), FO (CD19$^+$IgM^{lo}CD21^{lo}CD23^{hi}), MZ (CD19$^+$IgM^{hi}CD21^{hi}CD23^{lo}), or MZ-P (CD19$^+$IgM^{hi}CD21^{hi}CD23^{hi}) B cells were FACS sorted from mice that were injected with mOVA$^+$ apoptotic cells 30 min prior to sacrifice. In other experiments, sorted RPMs, FO, MZ, or MZ-P B cells (5×10^5 each) from naïve 2-mo-old BXD2 mice were cocultured with purified and CFSE (1 μM) labeled OT-II CD4 T cells (2×10^5) in the presence or absence of either OVA protein or OVA$_{323-339}$ peptide as described previously (15) In all *in vitro* experiments, CD4 T cell proliferative response was determined by the reduction of CFSE intensity by flow cytometry 3 d after coculture.

Reagents and Analyses

Flow cytometry and immunofluorescence microscopy were carried out as previously described (12). Real-time quantitative polymerase chain reaction (qRT-PCR) was carried out as described (12) using the following primers: *Il6*, TCCAGTTTGGTAGCATCCATC (F), CCGGAGAGGAGACTTCACAG (R); *Il10*, AATTCCCTGGGTGAGAAG (F), TGCAGTTGATGATGAAGATGTC (R); *Tgfb*: CTACTATGCTAAAGAGGTCAC (F), reverse CATGTTGCTCCACACTTG (R). For western blot analysis, anti-Btk (Santa Cruz),

anti-IDO (Abcam), anti-GAPDH, anti-SHIP1 and anti-rabbit HRP-conjugated Ab (Cell Signaling Technology) were used.

Results and Discussion

Reduction of MZMs in BXD2 mice

Confocal imaging (Fig. 1A) and FACS analysis (Fig. 1B) were used to determine the integrity and enumerate the percentage of SIGN-R1$^+$ MZMs in the spleens of autoimmune BXD2 mice. There was an age-dependent loss of MZMs in the BXD2 mice but not in the B6 mice (Fig. 1A, 1B). The total numbers of F4/80^{neg}CD11b^{lo}I-A^{bneg}SIGN-R1$^+$ MZMs (16) were equivalent in 3-mo-old B6 and BXD2 mice, but there was dramatic loss of these cells in 9-mo-old BXD2 but not B6 mice (Fig. 1B). There was an age-related defect in clearance of apoptotic cells as indicated by an increase in the number of TUNEL$^+$ apoptotic cells found near the MZMs and inside areas of the follicle distinct from the GCs in BXD2 mice (Fig. 1C). Consistent with these, there were age-related increases in the levels of circulating autoantibodies for MARCO, SR-A, and DNA in BXD2 mice (Fig. 1D). Elevation of IgG anti-MARCO and anti-SR-A was found in the serum of lupus patients and mouse models of lupus and these autoantibodies potentially affect macrophage phagocytosis of apoptotic cells (7).

Capture of apoptotic cell debris by B cells and their intra-follicular migration

The functional activities of the MZMs were evaluated by the ability to clear exogenous CFSE labeled apoptotic thymocytes (Fig. 2A). Compared to B6 mice, the apoptotic thymocytes persisted for an extended period of time in 2-mo-old BXD2 mice. Thus, the functional defects in the MZMs precede the loss of these cells and represent one of the earliest autoimmune defects detected in the BXD2 strain.

The failure to clear Ags alone is not, however, sufficient to induce an autoimmune response in BXD2 mice as large GCs are found inside the follicles. Cyster and colleagues have shown that B cells can shuttle between the MZ and FO areas thereby facilitating Ag transport (15). We have established previously that, in BXD2 mice, there is the expansion in number of MZ-P B cell which is associated with the reduction of the MZ B cells and also the heightened Ag delivery by MZ-P B cells (17, 18).

To determine if BXD2 B cells can capture and deliver apoptotic cell Ags in MZM-deficient conditions, we tracked CFSE-labeled apoptotic thymocytes in mice that were treated with 150 μg of CL. This dose was used because it selectively induced uptake of liposomes by MZMs (Supplemental Figure S1A). In mice administered CL, there was a time dependent capture of apoptotic cells by MZ B and MZ-P B, but not FO B cells (Fig. 2B and Supplemental Figure S1B). The numbers of CFSE$^+$ cells, which were located predominately in the MZ, peaked at 5–15 minutes and the majority was processed at 60 min (Fig. 2C, left). This may be associated with the higher uptake of CFSE by MZ, compared with MZ-P B cells during these early time points (Fig. 2B and Supplemental Figure S1B). Within 5 to 30 min, there was a rapid migration of MZ-P B cells to the periphery of the follicle and into the MZ (Fig. 2C, **right and** Supplemental Figure S1C, S1D). By 1 h after administration of the apoptotic cells, the majority of MZ-P, but not MZ B cells, exhibited massive inward migration into the follicles. At this time point, the majority of both the MZ-P and MZ B cells carried the apoptotic debris (Fig. 2B, 2C and Supplemental Figure S1B)

Apoptotic Ags capturing MZ-P B cells stimulate CD4$^+$ T cells

To determine if MZMs are mechanistically required to suppress the T-cell response to apoptotic cells and associated Ags, we transferred CFSE-labeled OT-II TCR transgenic T

cells into BXD2 and B6 mice and assessed the response of Vβ5^{+} T cells to apoptotic thymocytes derived from mOVA Tg mice. There were significantly higher numbers of OT-II T cells that entered the cell cycle in the spleens of the 2 and 9 mo BXD2 mice than the spleens of age-matched B6 mice post apoptotic mOVA[+] thymocyte transfer (Fig. 3A right). The percentages of CFSE-labeled OT-II T cells that entered the cell cycle in CL administered mice was similar to that observed in 9-mo-old BXD2 mice (Fig. 3A right), which is consistent with the dramatic loss of MZMs observed in the older BXD2 mice (Fig. 1A, 1B).

We previously have shown that the T-cell costimulatory function of MZ-P B cells is superior to other B cells in BXD2 mice (17, 18). We therefore cocultured CFSE-labeled OT-II CD4^{+} T cells with F4/80^{+} RPMs or subpopulations of B cells sorted from the spleens of BXD2 mice that had been administered mOVA thymocytes. These results show that both MZ and MZ-P B cells can present Ags derived from apoptotic cells, and this Ag presentation and stimulation of T cells is higher in BXD2 mice as compared to B6 mice (Fig. 3B and Supplemental Figure S2). Although the ability of MZ-P B cells to process intact OVA proteins for stimulation of CD4^{+} T cells was lower than that of RPMs, the ability of MZ-P B cells to present OVA peptide for stimulation of T cells was superior to that of all other tested B cell populations from BXD2 spleens (Fig. 3C). This suggests that MZ-P B cells that have migrated into the follicular region may either directly process or capture processed apoptotic cell Ags thereby stimulating CD4^{+} T cells.

Under normal conditions, phagocytic cells that ingest apoptotic cells produce tolerogenic signals, including TGFβ and IL-10, that maintain tolerance to self-Ags (19). Both MZMs and MZ-P B cells from 3-mo-old BXD2 mice exhibited lower expression of genes encoding tolerogenic cytokines, including TGF-β and IL-10, and higher expression of the gene encoding the immunogenic cytokine IL-6, compared to those from B6 MZMs and MZ-P B cells (Fig. 3D). Indoleamine 2,3-dioxygenase (IDO) has recently been shown to be an important tolerogenic signal inducer in MZMs of B6 mice following apoptotic cell administration (6). IDO, however, was detectable in MZMs of unmanipulated younger MRL-Fas*lpr/lpr* mice, and its inhibition with D-1-methyl-tryptophan (D1MT) promoted autoimmunity (6), suggesting that low IDO can enhance but is not the primary cause of autoimmunity in MRL-Fas*lpr/lpr* mice. In contrast, the present study demonstrated the first time that CD11b^{+} cells from a mouse model of spontaneous autoimmunity expressed significantly lower levels of IDO, compared to those from normal B6 mice (Fig. 3E). Also, local high levels of IL-6 might contribute to an immunogenic signal for apoptotic cell Ags as IL-6 degrades IDO (20). The TGF-β–IDO immunoreceptor tyrosine-based inhibitory motifs (ITIMs) stimulate SHIP-1 (*Inpp5d*) and the TGF-β–IDO–SHP axis has been identified recently as the major long-term tolerogenic signal in DCs (21). There also were dramatically lower levels of SHIP-1 together with higher levels of its counteracting molecule, Btk (9), in the CD11b^{+} cells from the spleens of the BXD2 mice (Fig. 3E). These findings are consistent with the observations that loss of the expression of SHIP-1 in myeloid cells of Lyz. Cre *Ship1*^{−/−} mice was associated disrupted MZM integrity and enhanced splenomegaly and that deficiency of Btk in Lyz. Cre *Ship1*^{−/−} mice reversed these phenotypes (9).

In summary, we have shown previously that the development of the high titers of autoantibodies in BXD2 mice is dependent on abnormalities in two different compartments in the spleen: (*i*) Enhanced production of type I interferons in the MZ induces follicular translocation of Ag-bearing MZ-P B cells which costimulate T cells (17, 18); and (*ii*) Enhanced IL-17 production in the GCs that upregulates regulator of G-protein signaling proteins thereby enhancing T-B cell interactions (12, 22). We now have observed that these abnormalities are anatomically preceded by the development of defects in the MZ barrier in

the BXD2 mice. Collectively, the present results suggest a novel mechanism of autoimmunity in which "leaks" in the follicular exclusion of self apoptotic Ags together with enhanced activity of carrier B cells subverts otherwise protected adaptive immune processes in the follicles. McHeyzer-Williams elegantly described the importance of B cells as initial Ag transporting cells in adaptive immunity (23). The present study directly demonstrates that in a situation in which MZM apoptotic debris ingestion and tolerogenic functions are defective, follicular translocating immunogenic B cells can capture and deliver the autoantigens into the follicles, thus providing the previously unknown bridging mechanism between defective clearance of apoptotic debris and the development of autoantibodies. Strategies that restore and retolerize MZM function may represent a novel approach to attenuation of autoimmune disease.

Supplementary Material

Refer to Web version on PubMed Central for supplementary material.

Acknowledgments

Abbreviations used in this article

AC	apoptotic cell
Btk	Bruton's tyrosine kinase
CL	clodronate liposome
FO	follicle or follicular
GC	germinal center
IDO	indoleamine 2,3-dioxygenase
mOVA	membrane bound chicken ovalbumin
MZM	marginal zone macrophages
MZ-P	marginal zone precursor B cells
RPM	red pulp macrophages
SHIP-1	SH2 domain-containing inositol 5′-phosphatase 1
Tg	transgenic

References

1. Casciola-Rosen LA, Anhalt G, Rosen A. Autoantigens targeted in systemic lupus erythematosus are clustered in two populations of surface structures on apoptotic keratinocytes. The Journal of experimental medicine. 1994; 179:1317–1330. [PubMed: 7511686]

2. Fransen JH, Hilbrands LB, Ruben J, Stoffels M, Adema GJ, van der Vlag J, Berden JH. Mouse dendritic cells matured by ingestion of apoptotic blebs induce T cells to produce interleukin-17. Arthritis Rheum. 2009; 60:2304–2313. [PubMed: 19644874]

3. Peng Y, Martin DA, Kenkel J, Zhang K, Ogden CA, Elkon KB. Innate and adaptive immune response to apoptotic cells. J Autoimmun. 2007; 29:303–309. [PubMed: 17888627]

4. Miyake Y, Asano K, Kaise H, Uemura M, Nakayama M, Tanaka M. Critical role of macrophages in the marginal zone in the suppression of immune responses to apoptotic cell-associated antigens. J Clin Invest. 2007; 117:2268–2278. [PubMed: 17657313]

5. McGaha TL, Chen Y, Ravishankar B, van Rooijen N, Karlsson MC. Marginal zone macrophages suppress innate and adaptive immunity to apoptotic cells in the spleen. Blood. 2011; 117:5403–5412. [PubMed: 21444914]

6. Ravishankar B, Liu H, Shinde R, Chandler P, Baban B, Tanaka M, Munn DH, Mellor AL, Karlsson MC, McGaha TL. Tolerance to apoptotic cells is regulated by indoleamine 2,3-dioxygenase. Proceedings of the National Academy of Sciences of the United States of America. 2012; 109:3909–3914. [PubMed: 22355111]

7. Chen XW, Shen Y, Sun CY, Wu FX, Chen Y, Yang CD. Anti-class a scavenger receptor autoantibodies from systemic lupus erythematosus patients impair phagocytic clearance of apoptotic cells by macrophages in vitro. Arthritis research & therapy. 2011; 13:R9. [PubMed: 21281474]

8. Wermeling F, Chen Y, Pikkarainen T, Scheynius A, Winqvist O, Izui S, Ravetch JV, Tryggvason K, Karlsson MC. Class A scavenger receptors regulate tolerance against apoptotic cells, and autoantibodies against these receptors are predictive of systemic lupus. The Journal of experimental medicine. 2007; 204:2259–2265. [PubMed: 17893199]

9. Karlsson MC, Guinamard R, Bolland S, Sankala M, Steinman RM, Ravetch JV. Macrophages control the retention and trafficking of B lymphocytes in the splenic marginal zone. The Journal of experimental medicine. 2003; 198:333–340. [PubMed: 12874264]

10. Mountz JD, Yang P, Wu Q, Zhou J, Tousson A, Fitzgerald A, Allen J, Wang X, Cartner S, Grizzle WE, Yi N, Lu L, Williams RW, Hsu HC. Genetic segregation of spontaneous erosive arthritis and generalized autoimmune disease in the BXD2 recombinant inbred strain of mice. Scand J Immunol. 2005; 61:128–138. [PubMed: 15683449]

11. Hsu HC, Wu Y, Yang P, Wu Q, Job G, Chen J, Wang J, Accavitti-Loper MA, Grizzle WE, Carter RH, Mountz JD. Overexpression of activation-induced cytidine deaminase in B cells is associated with production of highly pathogenic autoantibodies. Journal of immunology. 2007; 178:5357–5365.

12. Hsu HC, Yang P, Wang J, Wu Q, Myers R, Chen J, Yi J, Guentert T, Tousson A, Stanus AL, Le TV, Lorenz RG, Xu H, Kolls JK, Carter RH, Chaplin DD, Williams RW, Mountz JD. Interleukin 17-producing T helper cells and interleukin 17 orchestrate autoreactive germinal center development in autoimmune BXD2 mice. Nature immunology. 2008; 9:166–175. [PubMed: 18157131]

13. Hsu HC, Yang P, Wu Q, Wang JH, Job G, Guentert T, Li J, Stockard CR, Le TV, Chaplin DD, Grizzle WE, Mountz JD. Inhibition of the catalytic function of activation-induced cytidine deaminase promotes apoptosis of germinal center B cells in BXD2 mice. Arthritis Rheum. 2011; 63:2038–2048. [PubMed: 21305519]

14. Hsu HC, Zhou T, Kim H, Barnes S, Yang P, Wu Q, Zhou J, Freeman BA, Luo M, Mountz JD. Production of a novel class of polyreactive pathogenic autoantibodies in BXD2 mice causes glomerulonephritis and arthritis. Arthritis Rheum. 2006; 54:343–355. [PubMed: 16385526]

15. Cinamon G, Zachariah MA, Lam OM, Foss FW Jr, Cyster JG. Follicular shuttling of marginal zone B cells facilitates antigen transport. Nature immunology. 2008; 9:54–62. [PubMed: 18037889]

16. Taylor PR, Martinez-Pomares L, Stacey M, Lin HH, Brown GD, Gordon S. Macrophage receptors and immune recognition. Annu Rev Immunol. 2005; 23:901–944. [PubMed: 15771589]

17. Wang JH, Wu Q, Yang P, Li H, Li J, Mountz JD, Hsu HC. Type I interferon-dependent CD86(high) marginal zone precursor B cells are potent T cell costimulators in mice. Arthritis Rheum. 2011; 63:1054–1064. [PubMed: 21225691]

18. Wang JH, Li J, Wu Q, Yang P, Pawar RD, Xie S, Timares L, Raman C, Chaplin DD, Lu L, Mountz JD, Hsu HC. Marginal zone precursor B cells as cellular agents for type I IFN-promoted antigen transport in autoimmunity. Journal of immunology. 2010; 184:442–451.

19. Perruche S, Zhang P, Liu Y, Saas P, Bluestone JA, Chen W. CD3-specific antibody-induced immune tolerance involves transforming growth factor-beta from phagocytes digesting apoptotic T cells. Nat Med. 2008; 14:528–535. [PubMed: 18438416]

20. Pallotta MT, Orabona C, Volpi C, Grohmann U, Puccetti P, Fallarino F. Proteasomal Degradation of Indoleamine 2,3-Dioxygenase in CD8 Dendritic Cells is Mediated by Suppressor of Cytokine Signaling 3 (SOCS3). International journal of tryptophan research : IJTR. 2010; 3:91–97. [PubMed: 22084591]

21. Pallotta MT, Orabona C, Volpi C, Vacca C, Belladonna ML, Bianchi R, Servillo G, Brunacci C, Calvitti M, Bicciato S, Mazza EM, Boon L, Grassi F, Fioretti MC, Fallarino F, Puccetti P, Grohmann U. Indoleamine 2,3-dioxygenase is a signaling protein in long-term tolerance by dendritic cells. Nature immunology. 2011; 12:870–878. [PubMed: 21804557]

22. Xie S, Li J, Wang JH, Wu Q, Yang P, Hsu HC, Smythies LE, Mountz JD. IL-17 activates the canonical NF-kappaB signaling pathway in autoimmune B cells of BXD2 mice to upregulate the expression of regulators of G-protein signaling 16. Journal of immunology. 2010; 184:2289–2296.

23. McHeyzer-Williams LJ, Pelletier N, Mark L, Fazilleau N, McHeyzer-Williams MG. Follicular helper T cells as cognate regulators of B cell immunity. Curr Opin Immunol. 2009; 21:266–273. [PubMed: 19502021]
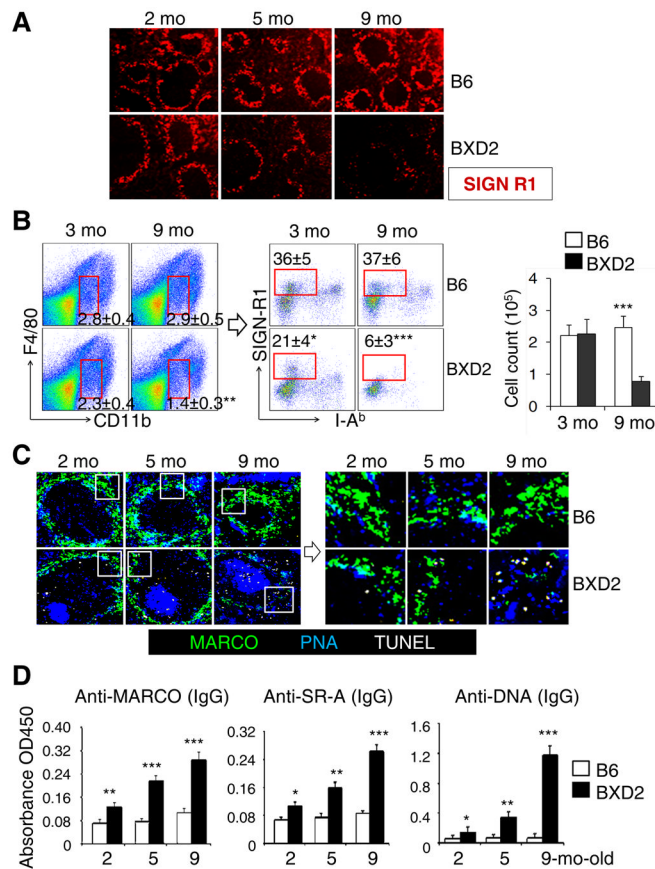
Figure 1.
Age-related decrease in MZMs in BXD2 spleens. (***A–C***) Naive B6 and BXD2 mice were sacrificed at the indicated age. (***A***) Confocal imaging showing the decline of MZMs in the spleen in BXD2 mice. (***B***) Left and Middle: FACS analysis showing the frequency of $CD11b^{int}F4/80^{lo}SIGN-R1^{+}I-Ab^{neg}$ MZMs (rectangle gated cells) in the spleen of B6 and BXD2 mice. Right: total MZM cell count was calculated by multiplying the percentage of MZMs by the total spleen cell count obtained from each mouse. (***C***) Left: Confocal imaging showing the anatomic location of apoptotic cells (TUNEL^{+}) relative to the location of MZMs (MARCO^{+}) and GCs (PNA^{+}) in the representative follicle; Right, A high power view of the boxed area from the left. (***D***) ELISA analysis of serum titers of the indicated autoantibodies in the indicated strains. All data are Mean ± standard error of the mean (SEM) (N=3–4 per group for 2 independent experiments; * p<0.05, ** p<0.01, *** p<0.005 between results from B6 and BXD2 of the same age).
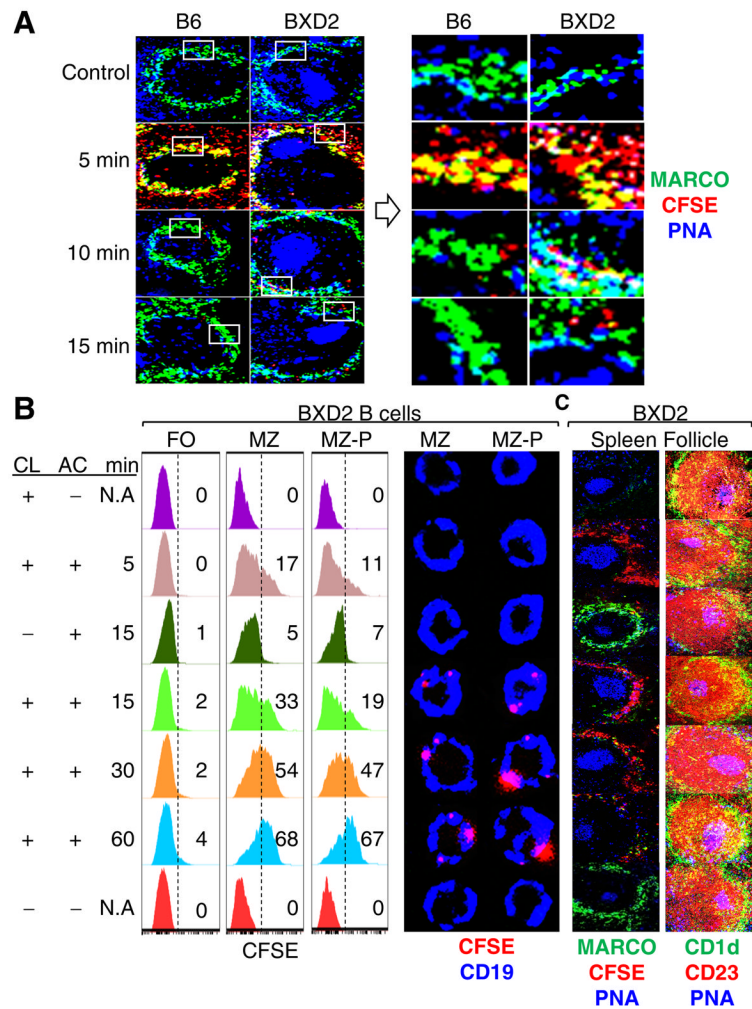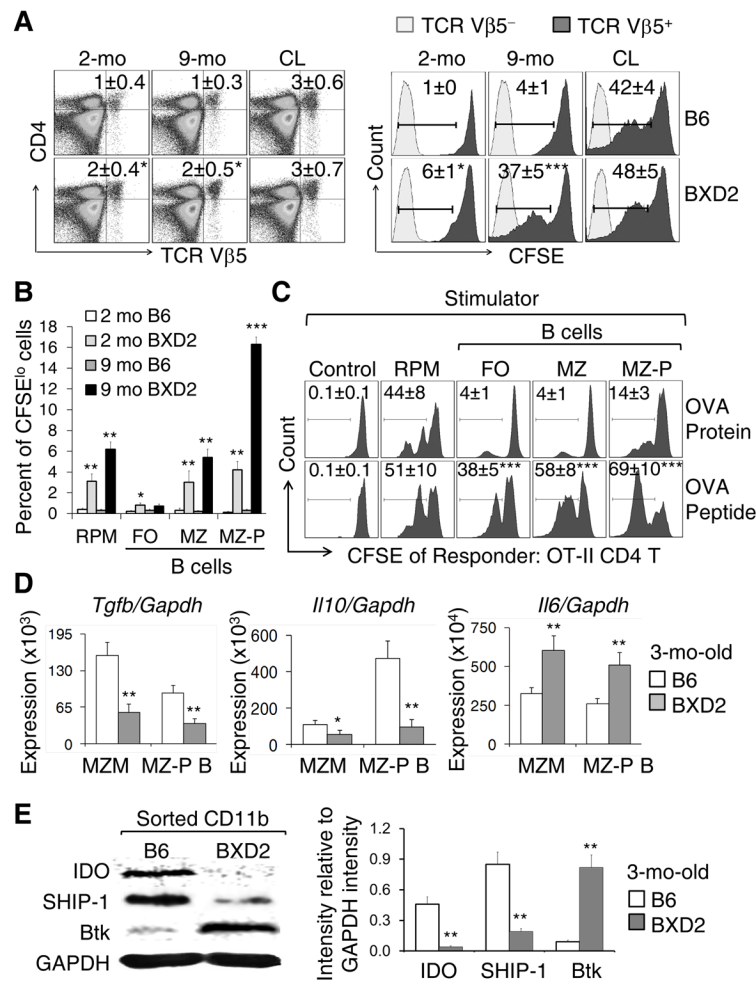
Figure 2.
Defective clearance of apoptotic debris is associated with increased uptake of apoptotic cells by MZ/FO shuttling MZ-P B cells in the spleens of BXD2 mice. (***A***) Left: Confocal imaging showing the kinetics of clearance of administered CFSE-labeled apoptotic thymocytes (pseudo color red) in the MZ area in the spleen of 2-mo-old mice. Right: High power view of the indicated (box) areas in the left panels. (***B, C***) BXD2 mice (2-mo) were treated with either CL- or PBS-liposome 4 hrs prior to CFSE-labeled apoptotic thymocyte administration. Following AC administration, mice were sacrificed at the indicated time points (min). (***B***) Left: FACS analysis of subpopulations of B cells that were positive for AC Ags (CFSE+). FO, MZ, and MZ-P B cells were gated as described (17, 18). Right: Confocal imaging assessment of the binding of FACS sorted MZ or MZ-P B cells with CFSE+ (pseudo color red) apoptotic debris. A representative cell from the indicated subset is shown. (***C***) Confocal imaging showing a representative spleen follicle from each group to reveal the clearance of the administered CFSE+ apoptotic thymocytes (pseudo color red) in the spleen (left) and the anatomic location of FO (red: CD1d− CD23+), MZ (green: CD1d+CD23−), MZ-P (yellow: CD1d+CD23+), and GC (blue: PNA+) in each group (right) (N=2–3 mice per group for 3 independent experiments).

Figure 3.
Stimulation of CD4 T cells by MZ-P B cells carrying apoptotic cell Ags. (*A*) Left: Flow cytometry analysis on the percentage of the transferred BXD2 OT-II CD4 T cells (TCR Vβ5) in the indicated recipient groups. Right: Flow cytometry analysis of the *in vivo* OVA-specific proliferative response of Vβ5$^+$ T cells, indicated by attenuation of CFSE intensity, of the transferred OT-II TCR CD4 T cells. Control mice (2-mo-old) were administered CL. (*B*) Bar graph analysis of the *in vitro* proliferative response OT-II TCR CD4 T cells (CFSE^{lo}) in response to the OVA Ag presented *in vivo* by the indicated cell populations. The indicated mOVA Ag bearing APCs were FACS sorted from the spleens of mice that have been administered apoptotic mOVA$^+$ thymocytes. (*C*) Flow cytometry analysis of the *in vitro* OT-II T cell proliferative response (CFSE^{lo}) to either OVA protein or the OVA$_{323-339}$ peptide processed or presented by the indicated populations of cells FACS sorted from naive 2-mo-old BXD2 mice. CSFE labeled OT-II T cell alone were used as control. (*D*) RT-PCR analysis of the expression of indicated gene in sorted MZMs and MZ-P B cells derived from the spleen of naive mouse. (*E*) Left: Western blot analysis of the expression of indicated protein in sorted CD11b cells from naive mice. Right, ImageJ analysis of the intensity of each protein after normalization with the intensity of GAPDH (N=3–4 per group; *$p < 0.05$; **$p < 0.01$; ***$p < 0.005$ compared with the same population of cells from B6 mice for *A*, *B*, *D*, *E* or from OVA protein stimulated cells for *C*).